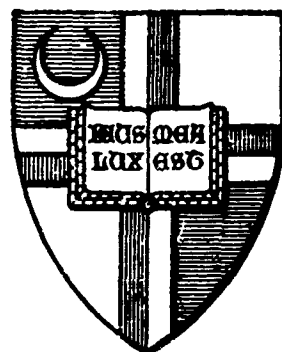
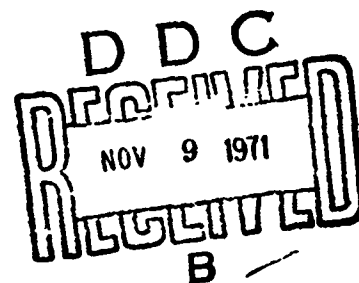


AD 732007

Institute of Ocean Science and Engineering  
The Catholic University of America  
Washington, D.C. 20017

Reproduced by  
NATIONAL TECHNICAL  
INFORMATION SERVICE  
Springfield, Va 22151

DISTRIBUTION STATEMENT A  
Approved for public release;  
Distribution Unlimited



28

Security Classification

**DOCUMENT CONTROL DATA - R & D**

*(Security classification of title, body of abstract and indexing annotation must be entered when the overall report is classified)*

1. ORIGINATING ACTIVITY (Corporate author) The Institute of Ocean Science and Engineering The Catholic University of America Washington, D.C. 20017		2a. REPORT SECURITY CLASSIFICATION <b>Unclassified</b>	
		2b. GROUP	
3. REPORT TITLE Analysis of the Operating Characteristics of Strands in tension allowing end rotation			
4. DESCRIPTIVE NOTES (Type of report and inclusive dates) Institute of Ocean Sciences and Engineering      Report 71 - 10			
5. AUTHOR(S) (First name, middle initial, last name)  Michael Chi			
6. REPORT DATE August 10, 1971		7a. TOTAL NO. OF PAGES 25	7b. NO. OF REFS 11
8a. CONTRACT OR GRANT NO. N00014 - 68 - A - 0506 - 0001		9a. ORIGINATOR'S REPORT NUMBER(S) Report 71 - 10	
b. PROJECT NO			
c.		9b. OTHER REPORT NO(S) (Any other numbers that may be assigned this report)	
d.			
10. DISTRIBUTION STATEMENT Distribution of this document is unlimited			
11. SUPPLEMENTARY NOTES		12. SPONSORING MILITARY ACTIVITY Office of Naval Research Department of the Navy	
13. ABSTRACT  A rational analysis of wire strand in tension is made through the use of exact geometrical relationship and theory of mechanics of materials. The calculated strains, deformations and end-rotations of a strand agree well with the experimental data. Effect of the end-rotation on the load distribution in the wires of a strand is shown in detail. It was also found that the gap between the core and helical wires had a surprisingly high effect on the load distribution in the wires and the amount of end-rotation. The present construction of strands is critically analyzed and possible improved design is indicated. Finally, a truly non-spinning strand design is presented on the basis of this new method of analysis.			

**DD FORM 1473** (PAGE 1)  
1 NOV 65

S/N 0101-807-6801

Security Classification

14

KEY WORDS

LINK A

LINK B

LINK C

ROLE

WT

ROLE

WT

ROLE

WT

strand, rope

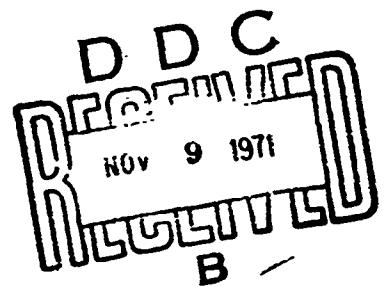
ANALYSIS OF OPERATING CHARACTERISTICS OF STRANDS  
IN TENSION ALLOWING END-ROTATION

by

MICHAEL CHI

Department of Civil & Mechanical Engineering

Report 71-10  
N00014-68-A-0506-0001  
September 1971



## ABSTRACT

A rational analysis of wire strand in tension is made through the use of exact geometrical relationship and theory of mechanics of materials. The calculated strains, deformations and end-rotations of a strand agree well with the experimental data. Effect of the end-rotation on the load distribution in the wires of a strand is shown in detail. It was also found that the gap between the core and helical wires had a surprisingly high effect on the load distribution in the wires and the amount of end-rotation. The present construction of strands is critically analyzed and possible improved design is indicated. Finally, a truly non-spinning strand design is presented on the basis of this new method of analysis.

## INTRODUCTION

The widespread use of wire strands and ropes in industry demands a constant updating of the knowledge of the design and construction. Today, a large selection of strands and ropes are available for various field applications[1]. To select a proper type of ropes for a specific job, the designer must be thoroughly familiar with their operating characteristics. This paper deals with one of these - the behavior of a multi-wire strand subjected to an axial tension.

Method of stress analysis of strands and ropes was presented by Hruska[2,3,4]. More recent investigators, with possible exception of Starkey and his students[5,6], still essentially follow his approach [7,8]. However, his method was based on the assumptions that the deformation and end-rotation are small and the radius of the strand or rope remains constant during loading. These assumptions are perhaps valid for steel strands and ropes having solid cores and, for strands and ropes of moderate lengths, the calculated stresses and deformations are perhaps adequate for practical purposes. In the modern technology, synthetic fiber ropes are used extensively; even for steel ropes, the core is usually made of fiber; for deep ocean studies, steel ropes as long as 15,000 feet are in common use. For these applications a more precise method of analysis should be developed to accurately predict its behavior.

## GEOMETRY OF A STRAND

A strand is made of a single, straight core wire wrapped around by one or more layers of helical wires. The total number of wires in a strand is  $3m(m+1)+1$ , where  $m$  is the number of layers. One-layered strand is called the guy strand or prestressing strand while that has two or more layers, the bridge strand. The helical wires in each layer make a constant angle,  $\alpha$ , with the section of the strand. The distance of one

lay is called the pitch and is denoted by  $p$ . The total length of the strand, which is the same as the length of the core wire, is denoted by  $L$ . The number of turns of the helical wires are denoted by  $n$  and are equal to  $L/p$ . The radius of the strand is defined as the distance from the axis of the strand to the center of a helical wire and is denoted by  $R$ . The arc length of a helical wire is denoted by  $S$ .

When a tensile load  $P$  is applied to the strand, its length is increased by  $\delta$  and, at the same time, if it is not restricted from turning, the end of the strand also unlays by an angle  $\phi$ . Geometrical consideration leads us to conclude that a helix describes a developable surface and the developed surface is a triangle OAB (Fig. 1).

After the load  $P$  is applied the developed surface becomes the triangle OA'B'. We shall use the primed symbols for deformed state throughout. The undeformed and the deformed lengths of the helical wire are, respectively,

$$S = \frac{L}{\sin \alpha}$$

$$S' = \frac{L + \delta}{\sin \alpha'}$$

$$\text{where } \sin \alpha' = \frac{L + \delta}{\sqrt{(L + \delta)^2 + R'^2 (L \cot \alpha / R - \phi)^2}} \quad (1)$$

The tensile strain in the helical wire is

$$\epsilon_h = \frac{S' - S}{S}$$

$$= \sin \alpha \sqrt{(1 + \epsilon_c)^2 + (K_1 \cot \alpha - R' \phi / L)^2} - 1 \quad (2)$$

where  $\epsilon_c = \delta/L$  = tensile strain in the core wire and

$$K_1 = \frac{R'}{R}$$

We note in passing that Eq. (2) is an exact geometrical relation between the engineering strains in the helical and core wires, valid for any number of layers in the strand, any lay angle and any amount of end-rotations of the strand. It is interesting to demonstrate that this expression includes previously available results as special cases. For instance, setting  $K_1 = 1$  and  $\phi = 0$ , we reduce Eq. (2) to

$$\epsilon_h = \sin \alpha \sqrt{(1 + \epsilon_c)^2 + \cot^2 \alpha} - 1$$

Using binomial expansion and retaining only the first order term, we obtain

$$\epsilon_h \sim \epsilon_c \sin^2 \alpha \quad (2A)$$

which is the relation first postulated by Griffith and Bragg [9] and derived by Hruska [2]. Essentially the same relationship has been the basis of the extensive application to the stress analysis of strands and ropes at least up to 1969 (5,6,7,8).

To include the effect of end-rotation we retain the term involving  $\phi$  in Eq. (2). By a similar procedure as above, we obtain,

$$\epsilon_h \sim \sin^2 \alpha \left( \epsilon_c - \frac{R'\phi}{L} \cot \alpha \right) \text{ to the first approximation} \quad (2B)$$

which is the same as the result by Hruska [4], using an elementary approach.

Solving for  $\epsilon_c$  in Eq. (2) and setting  $\epsilon_h$  and  $K_1$  to zero and unity, respectively, we have, by a similar procedure

$$\epsilon_c \sim \frac{R'\phi}{L \tan \alpha} \quad \text{or} \quad \delta \sim R'\phi \cot \alpha \quad (2C)$$

which was obtained also by Hruska [4] for a rigid rotation of the helical wire.

For any fixed values of  $K_1$  and  $\alpha$ , Eq. (2) can be used to determine the relation between  $\epsilon_h$  and  $\epsilon_c$  using  $\frac{R'\phi}{L}$  as a parameter. Fig. 2 shows such plots with  $K_1 = 1$  and  $\alpha = 82^\circ 43'$ , which is typical for a 5/16-in. steel strand. We see that these curves are very nearly straight lines having a slope approximately equal to



$\sin^2 \alpha$ , as indicated by Eqs. (2B).

We note also that the above discussion is valid for any layer of helical wires in a strand with reference to the core wire. There is no restriction of the number of layers. Of course,  $R'$  and  $\alpha$  may be different from one layer to the next and the outcome of Eq. (2) would also be different.

#### EQUATIONS OF EQUILIBRIUM

Now we proceed to write down the equilibrium equations for a **prestressing** strand. Let  $N$  be the number of helical wires and  $P_c$  and  $P_h$  are the resultants in the core and the helical wires, respectively. The equilibrium of loads requires that

$$P_c + NP_h \sin \alpha' = P \quad (3)$$

The equilibrium of moments requires that

$$M = N (M_b \cos \alpha' + M_t \sin \alpha') + M_c \quad (4)$$

where  $M$  = applied torsion, which, following Hruska [4], can be determined by the following:

$M = NP_h R' \cos \alpha'$ , as modified with the consideration of changing radius and pitch, and

$M_b$  = bending moment in each helical wire

$M_t$  = torsional moment in each helical wire and

$M_c$  = torsional moment in the core wire.

The first quantity above is the product of flexural rigidity and the change of curvature and can be shown to be the following:

$$M_b = E I_h \left( \frac{\cos^2 \alpha}{R} - \frac{\cos^2 \alpha'}{R'} \right) \quad (5)$$

where  $I_h$  = moment of inertia of the helical wire and

$E$  = Young's modulus

The other two quantities are the product of the torsional constant and the angle of twist or change of torsion, whichever the case may be. It can be shown that

$$M_t = G J_h \left( \frac{\cos \alpha \sin \alpha}{R} - \frac{\cos \alpha' \sin \alpha'}{R'} \right) \quad (6)$$

$$M_c = \frac{G J_c \phi}{L} \quad (7)$$

where  $J_h$  and  $J_c$  are the polar moments of inertia of the helical and core wires, respectively and  $G$  is the shear modulus.

#### METHOD OF SOLUTION

Eqs. (2), (3), and (4) can be solved for the unknowns  $P_h$ ,  $P_c$  and  $\phi$ , with the considerations of Eqs. (2), (5), (6), and (7). Unfortunately, these are non-linear, transcendental, implicit algebraic equations. No general procedure is available for its analytical solution. We therefore resort to a graphical method.

For greater generality, we cast Eqs. (3) and (4) in nondimensional form as follows:

$$K_2 \epsilon_c + \left( \frac{N A_h}{A_c} \sin \alpha' \right) = \frac{P}{A_c E} \quad (8)$$

$$(1 + \nu) (K_1 \cos^2 \alpha - \cos^2 \alpha') + (K_1 \cos \alpha \sin \alpha - \cos \alpha' \sin \alpha') \tan \alpha' + \left( \frac{J_c}{J_h} \right)^2 \frac{1}{N \cos \alpha'} \frac{R' \phi}{L} = \frac{P_h R'^2}{G J_h} \quad (9)$$

where  $A_h$  and  $A_c$  are the cross-sectional areas of the helical and core wires, respectively,  $K_2$  is a constant which is equal to 1 if there is a core wire and equal to zero for a hollow core and  $\nu$  = Poisson's ratio.

Fig. 3 shows the plots of  $\frac{P}{G} \frac{h R'^2}{J_h}$  vs.  $\epsilon_c$ , having  $\frac{R' \phi}{L}$  as parameter and with

prescribed values of  $K_1$ ,  $\alpha$ ,  $N$  and  $J_c/J_h$ . We note that curves are again very nearly straight lines, having a very flat slope. This shows that, at least for the constants used in this case, the end rotation is roughly proportional to  $\frac{P R'^2}{G J_h}$ . Since the latter is, in turn, proportional to  $\epsilon_h$ , we can conclude that  $\phi$  is also roughly proportional to  $\epsilon_h$ . This is not surprising, inasmuch as  $M$  is proportional to  $P_h$ . We have labeled  $\epsilon_h$  on the ordinate in Fig. 3, suitable for the 5/16-in. strand.

Now we proceed to discuss the proposed graphical method. For definiteness, suppose we choose the following problem:

Specimen = 5/16 in., steel, 7 - wire strand.

Diameter of core wire = 0.145 in.

Diameter of helical wire = 0.140 in.

Pitch (lay) = 7 in.

Length = 36 in.

Load = 5000 lb.

From the above data, we can plot Eq. (8) in both Figs. 2 and 3 as the "solution lines". The correct results must lie on these lines and also must be compatible in  $\epsilon_c$ ,  $\epsilon_h$  and  $R' \phi/L$ . From Fig. 2 with the consideration of the solution curve in it, we cannot be sure about either  $\epsilon_c$  nor  $R' \phi/L$  since they can vary in wide range. However, we are certain that  $\epsilon_h$  should not differ much from 0.0015.

With this value for  $\epsilon_h$ , the solution curve in Fig. 3 leads us to conclude that  $\epsilon_c$  and  $R' \phi/L$  must be 0.00195 and 0.0032, respectively. Using the latter two values, we go back to Fig. 2 to find the corresponding value of  $\epsilon_h$ . Continuing this process we obtain finally,

$$\begin{aligned}\epsilon_h &= 0.00149 \\ \epsilon_c &= 0.00195 \\ \frac{R' \phi}{L} &= 0.0032\end{aligned}$$

from which, the following can be determined,

$$\begin{aligned}P_h &= 678 \text{ lb.} \\ P_c &= 920 \text{ lb.} \\ \phi &= 0.807 = 46.2^\circ \\ \delta &= 0.0737 \text{ in.}\end{aligned}$$

The last value includes a "structural stretch" of 0.0001 per in. as determined experimentally. From Eq. (1) we can also compute  $\sin \alpha'$  and then, from Eq. (5), we found that  $M_b$  is 3.91 lb-in. which produces a flexural strain in the helical wire by the amount of  $\pm 0.0049$ . Combining the flexural strain and  $\epsilon_h$  shown above we see that the strains in the helical wire, due to combined bending and tension, vary from 1980 down to 1000 micro-in. per in. In addition,  $M_t$  is determined to be 10.1 lb-in. The corresponding shearing strain is 1660 micro-in. per in.

## VALIDATION OF THEORY

Tests have been carried out by Dr. Durelli and his associates [10] on a 5/16-in. strand and the experimental results are shown in Figs. 4, 5, and 6. The theoretical results are also presented there for comparison purposes. Fig. 4 shows the relation between load and deformation and the theoretical and experimental results are in a reasonable agreement. Fig. 5 shows the relation between load and longitudinal strains in helical wires. The strain gages were mounted approximately where the minimum combined strains are expected to occur. The measured strains show a considerable scatter and differ from wire to wire. Nevertheless, the analytical results run approximately through the mean value of the data from six gages. Fig. 6 shows the relation between loads and end-rotations. It is seen that the theoretical values are in good agreement with the experimental results.

Because of the agreement between the analytical and the experimental results and the proper degeneration of Eq. (2) into the known results in the literature as shown in the last section, we have considerable confidence on the theory given above. In the following we shall apply the theory to obtain new results which may be interesting and useful.

## APPLICATIONS

1. Effect of the end rotation on the stress distribution among wires.

It is well-known that the end rotation has a profound effect on the allocation of loads between the helical and the core wires. Some calculations to this effect were made both for strands and for wire ropes [4, 7, 8]. Fig. 7 shows in detail the variation of the strain in the helical wires of a strand vs. pitch angles with  $R'\phi/L$  as a parameter. It is seen that, for a fixed level of the strain in the core wire, and for a fixed pitch angle, the strain in the helical wires in general decreases with an increase of  $\frac{R'\phi}{L}$  and the former can be made to vanish at a moderate end rotation; in other words, at certain combinations of

parameters the load  $P$  can be made to apply only to the core wire and the helical wires are free from direct tension. The effect of end rotation is more pronounced for small pitch angles and, as the angle increases, the effect of end rotation diminishes steadily. When the pitch angle is very nearly  $90^\circ$ , however, rotation may produce an increase in the tensile strains in the helical wires, exceeding that in the core wire.

Fig. 8 is a typical chart which shows the variation of the strains in the helical and core wires at different load levels. It clearly shows that, at least for the factors considered therein, a moderate amount of end rotation can increase the strains in the core wire by as much as 80%. It is interesting to note that the end rotation also causes a slight decrease of the strains in the helical wires. This implies that the end rotation should also reduce the twisting moment somewhat and the bending moment and torsional moment in the helical wires must also be reduced accordingly.

2. Effect of reduction in the radius of the strand on the stress distribution between the wires.

We remark here that the radii of a strand in the deformed and undeformed states are not usually the same. The reduction in radius may be induced by any combination of three causes: (1) There is usually a small gap between the helical and core wires of a strand in the unloaded state such that a thin paper can be slipped through; (2) the elongation of the helical wire tends to decrease the radius of the helix, especially for a strand with a hollow or a soft core; (3) the tensile strains in the core and the helical wires tend to reduce the radii of these wires due to Poisson's effect. All three causes can easily produce a reduction in radius of the order of a few thousandths of an inch; in other words,  $K_1$  is usually appreciably lower than unity and may produce a considerable effect in the relative strains in the core and helical wires. To show this, we expand the radical in Eq. (2), keeping the linear term as before and obtain:

$$\epsilon_h \sim \epsilon_c \sin^2 \alpha - \frac{1 - K_1^2}{2} \cos^2 \alpha ; \phi = 0 \quad (2C)$$

If the effect of a small rotation is also included, we obtain, by a similar procedure, the following:

$$\epsilon_h \sim \epsilon_c \sin^2 \alpha - \frac{1 - K_1^2}{2} \cos^2 \alpha - \frac{K_1 R' \phi}{L} \sin \alpha \cos \alpha \quad (2D)$$

Eq. (2D) can be used for small  $\epsilon_c$  and  $\frac{R' \phi}{L}$ . It is not applicable to the plastic and fiber strands, of which either or both may be large. Setting  $K_1$  to unity in Eq. (2D), it reduces to Eq. (2B) which is valid only for rigid core with no initial gap.

We have made extensive calculations about this effect. Typical results are shown in Fig. 9 where we see that the ratio of radii have a surprisingly high effect on the strain in the strands. For any given  $\epsilon_c$ , a 10% reduction in radius, a reduction of the strand can reduce the strain in the helical wires by 50%.

### 3. Effect of number of helical wires on the tensile response of a strand.

Traditionally, a one-layer strand has six helical wires surrounding the core wire. It is interesting to investigate whether this is an optimum solution from the point of view of structural mechanics.

We shall use the 5/16-in. seven-wire strand described previously as the reference. The alternative constructions shall have the same pitch angle and same amount of metallic volume per unit length as the reference strand, except that the number of the helical wires can vary from five to twelve. The diameters of the helical and core wires, for constructions with  $N = 5$  through 12, turn out to be:

N	5	6	7	8	9	10	11	12
$d_h$	0.1582	0.1395	0.1254	0.1136	0.1037	0.0954	0.0883	0.0821
$d_c$	0.1157	0.1450	0.1688	0.1885	0.2050	0.2187	0.2306	0.2408

Unit: inch

When the strands having diameters of wires as shown above are loaded by the same tensile load  $P$  (5,000 lb.), their response can be determined by the same method as before. It is obvious that Eq. (2) stays unchanged but Eqs. (8) and (9) change considerably due to the variation of  $N$  and the cross-sectional areas of the wires. The details need not be elaborated here and we merely list the results as follows:

N	5	6	7	8	9	10	11	12
$\epsilon_h$	0.00154	0.00149	0.00147	0.00144	0.00143	0.00142	0.00142	0.00142
$\epsilon_c$	0.00185	0.00195	0.00191	0.00187	0.00185	0.00180	0.00174	0.00173
$\phi_{R/L}$	0.0023	0.0033	0.0033	0.0032	0.0030	0.0030	0.0023	0.0020

For the above it is seen that the strain in the helical wire decreases monotonically by a small amount as  $N$  increases, but is virtually asymptotic to a constant value for  $N$  greater than 9. The spread of strains, i.e.,  $(\epsilon_c - \epsilon_h)$ , is widest for  $N = 6$ , at 0.00036 and narrowest for  $N = 12$ , at 0.00031. The strain in the core wire and the end rotation are plotted in Figs. 10 and 11, respectively. We see that both of them increase as  $N$  increases from 5 and reach maxima between  $N = 6$  and 7 and then both of them decrease steadily for higher  $N$ .

From the above results we see that among all alternatives the seven-wire strand has the widest spread of strains among the wires, the largest elongation and the largest amount of end-rotation. If the criteria of "superior" construction of a strand are as follows:



- (1) As nearly uniform distribution of stress among the wires as possible.
- (2) As high an effective modulus of elasticity as possible.
- (3) As small an end rotation as possible,

then the seven-wire strands are close to the worst possible in performance.

To be fair to the strand manufacturers, there are other factors which must also be considered in the selection of a strand, such as the flexibility, durability, fatigue and corrosion, etc., to which we are <sup>not</sup> addressed. It is also true that seven-wire strands are used primarily as guy strands and prestressed concrete tendons, of which the ends are prevented from rotation so that the above discussion is not strictly applicable.

#### 4. Design of Non-spinning Strands.

For many engineering applications, including deep-ocean work, a truly non-spinning construction is desirable. Needless to say, all seven-wire strands have end-rotation. So let us try to modify the nineteen-wire bridge strand. This strand consists of 2 layers of helical wires of the same size. In order to be non-spinning these two layers must have opposite lays. Since the inner layer produces a much smaller twisting moment, the pitch angle should be chosen such that a maximum twisting moment is delivered. It can be easily shown that the desired pitch angle is  $54^{\circ}45'$ .

For definiteness, let us assume the diameter of helical wires be 0.14 in. and  $\epsilon_c$  be 0.006. We can compute the twisting moment due to the inner layer by the following expression:

$$M_{t1} = (\epsilon_{h1} A_h E) 6 R_1 \cos \alpha_1$$

where  $\epsilon_{h1}$  = strain in inner layer helical wires, which can be determined by Eq. (2).

$R_1$  = radius of strand measured to the inner layer = 0.1425 in.

In order that the strand is non-spinning, this moment must be balanced by the twisting moment produced by the outer layer.

The latter can be expressed by

$$M_{t2} = (\epsilon_{h2} A_c E) 12 R_2 \cos \alpha'_2$$

in which the subscripts 2 indicate the quantities referring to the outer layer.

By a trial and error method using Eq. (2), we obtain the unknowns as follows:

$$\epsilon_{h2} = 0.00591$$

$$\cos \alpha'_2 = 0.0985 \text{ or } \alpha'_2 = 84^\circ 21'$$

We believe that the construction suggested here is feasible for manufacturing.

Comparing with the conventional construction, the modified design requires of slightly larger metallic volume per unit length, which is believed to be a small price to pay for such a desirable property as non-spinning, provided, of course, that the scheme which looks good on paper, work out well in practice.

#### CONCLUDING REMARKS

The method presented in this paper appears to be accurate enough for practical purposes. Various applications are touched upon to illustrate its usefulness. A more systematic study for each application indicated above would undoubtedly enhance the understanding of the behavior of the wire strands.

Perhaps more importantly, the method should be extended to the structural analysis of wire rope, in which more variables are involved and the situation becomes much more complex. Ultimately, a viscoelastic analysis of plastic fiber wire ropes, in somewhat more refined manner than the pioneer work by Paul [11] should be a very rewarding undertaking.

## REFERENCES

1. For example, USS Tiger Brand Wire Rope Engineering Handbook, U. S. Steel Corporation, Pittsburgh, Pa., 1968.
2. Hruska, F. H., "Calculation of Stresses in Wire Ropes", Wire and Wire Products, Vol. 26, pp. 766-7, 799-801, September 1951.
3. Hruska, F. H., "Radial Forces in Wire Ropes", Wire and Wire Products, Vol. 27, pp. 459-463, May 1952.
4. Hruska, F. H., "Tangential Forces in Wire Rope", Wire and Wire Products, Vol. 28, pp. 455-460, May 1953.
5. Leissa, A. W., "Contact Stresses in Wire Ropes", Wire and Wire Products, Vol. 34, pp. 297-314, 372-3, March 1959.
6. Starkey, W. L., and Cress, H. A., "An Analysis of Critical Stresses and Mode of Failure of a Wire Rope", Journal of Engineering for Industry, ASME, pp. 307-316, November 1959.
7. Bert, C. W., and Stein, R. A., "Stress Analysis of Wire Rope in Tension and Torsion", Wire and Wire Products, Vol. 37, pp. 769-770, June 1962.
8. Gibson, P. T., Cress, H. A., and Kaufman, W. J., Gallant, W. E., "Torsional Properties of Wire Rope", ASME paper, 69-DE-34, May 5-8, 1969.
9. Griffith, J. H., and Bragg, J. G., "Strength and Other Properties of Wire Rope", Technologic Papers of the Bureau of Standards, No. 121, July 16, 1919.
10. Private communication from Dr. August J. Durelli.
11. Paul, W., "Review of Synthetic Fiber Ropes", R & D Project, U. S. Coast Guard Academy, New London, Conn., August 1970.

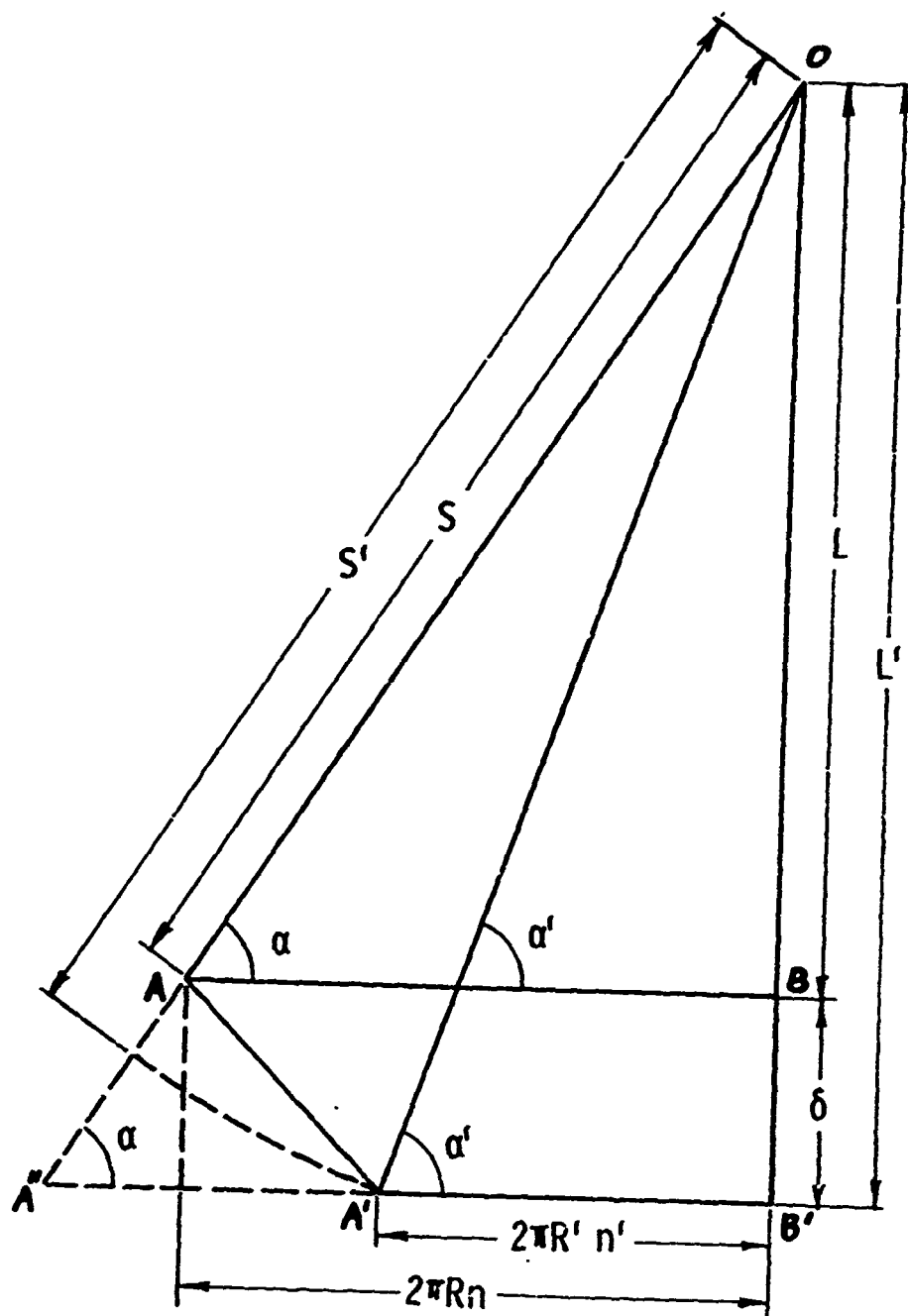


Fig. 1 Developed Surfaces in Deformed and Undeformed States

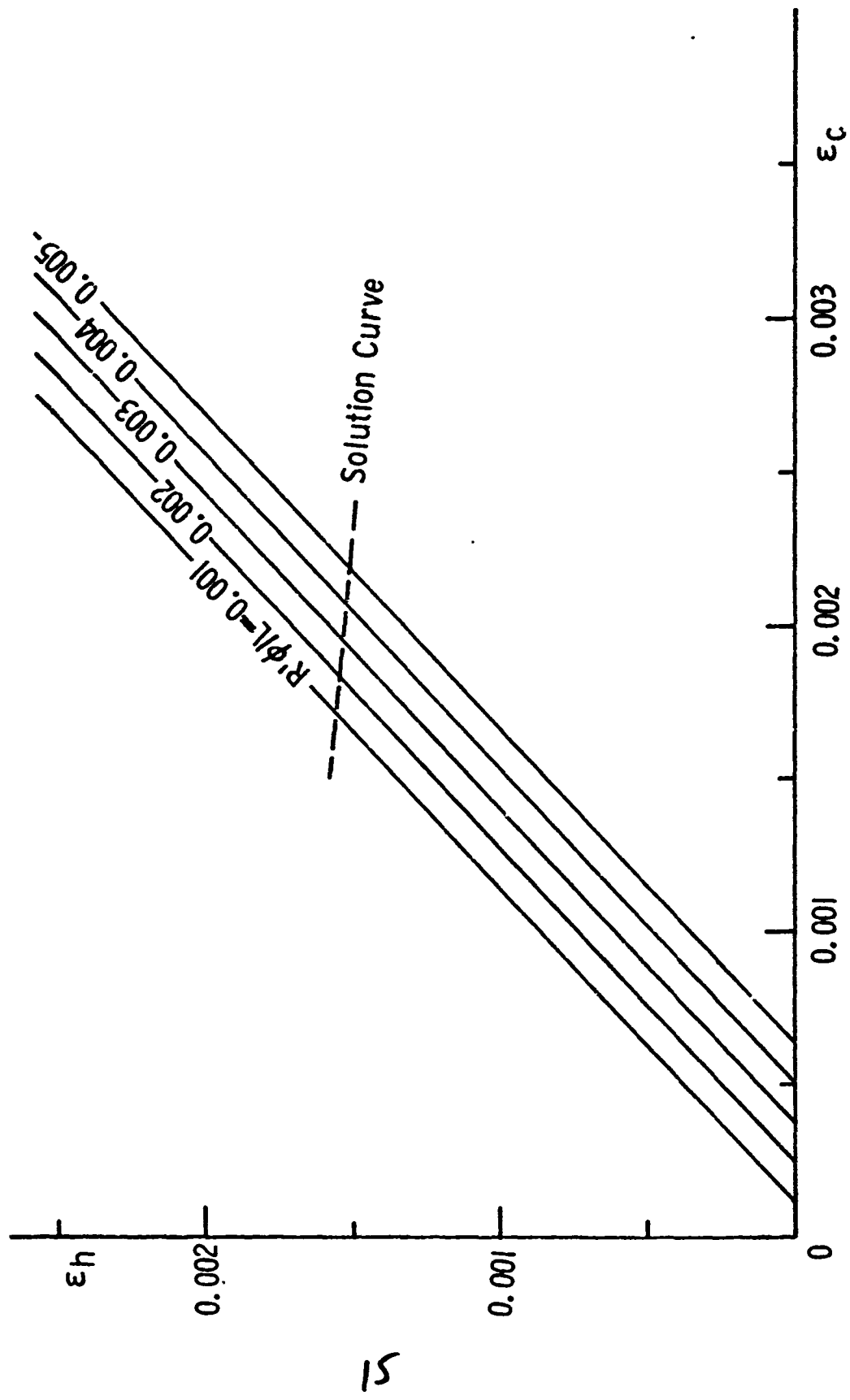


Fig. 2  $\epsilon_h$  vs.  $\epsilon_c$  in a 5/16-in. Strand for  $K_1 = 1$ .

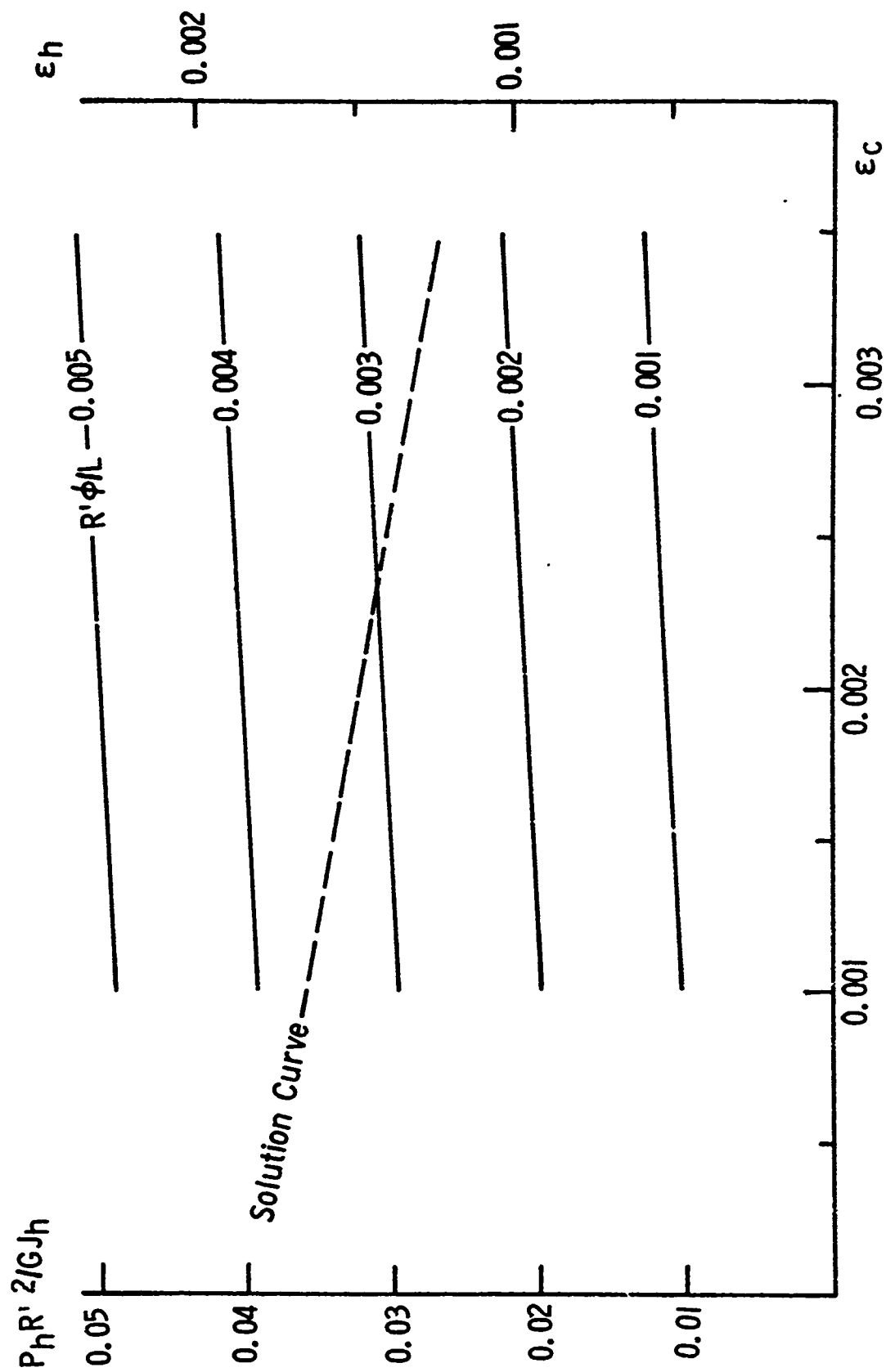


Fig. 3 Nondimensional Moment vs.  $\epsilon_c$  in a 5/16-in. Strand

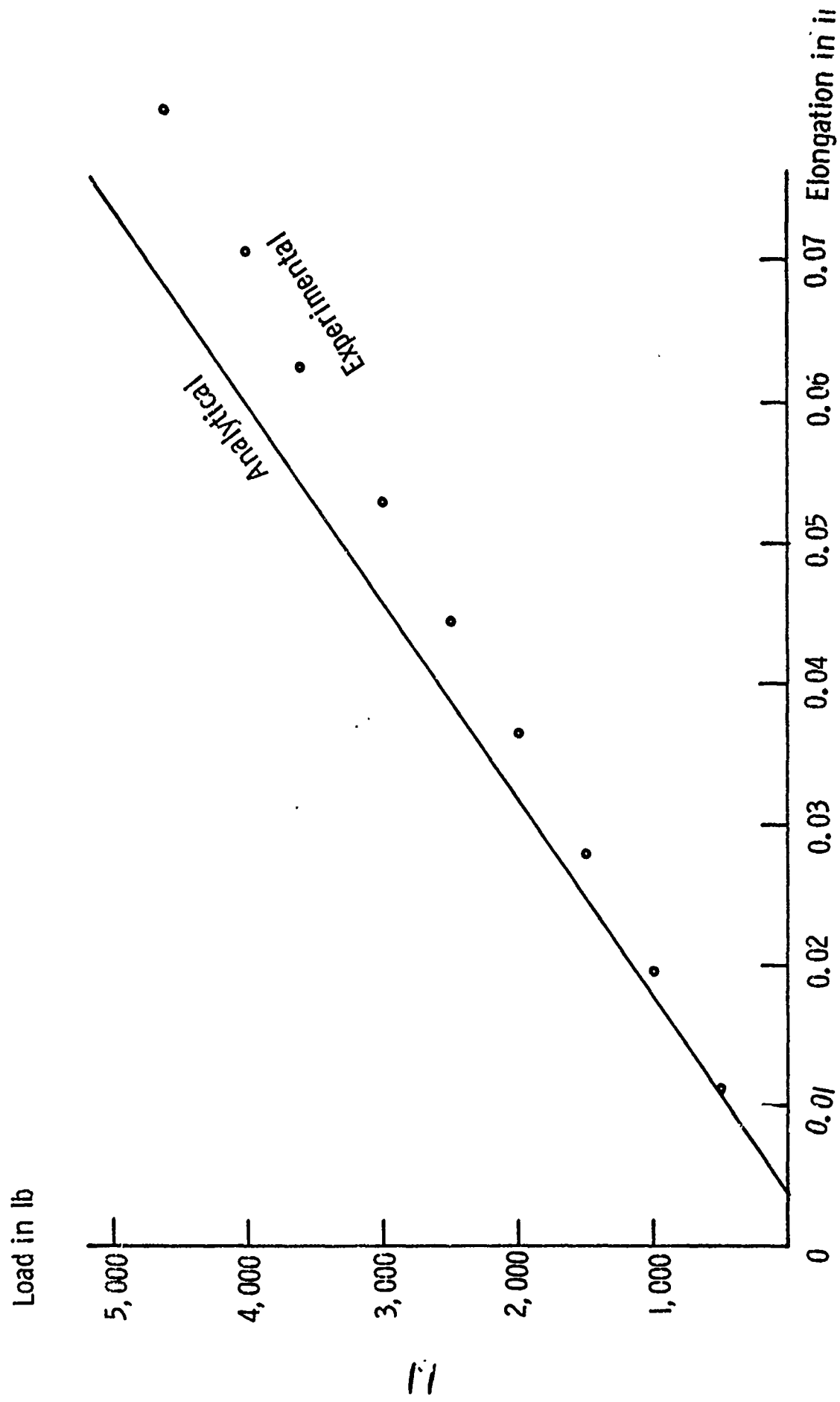


Fig. 4 Load vs. Elongation in a 5/16-in. Strand with Free-End

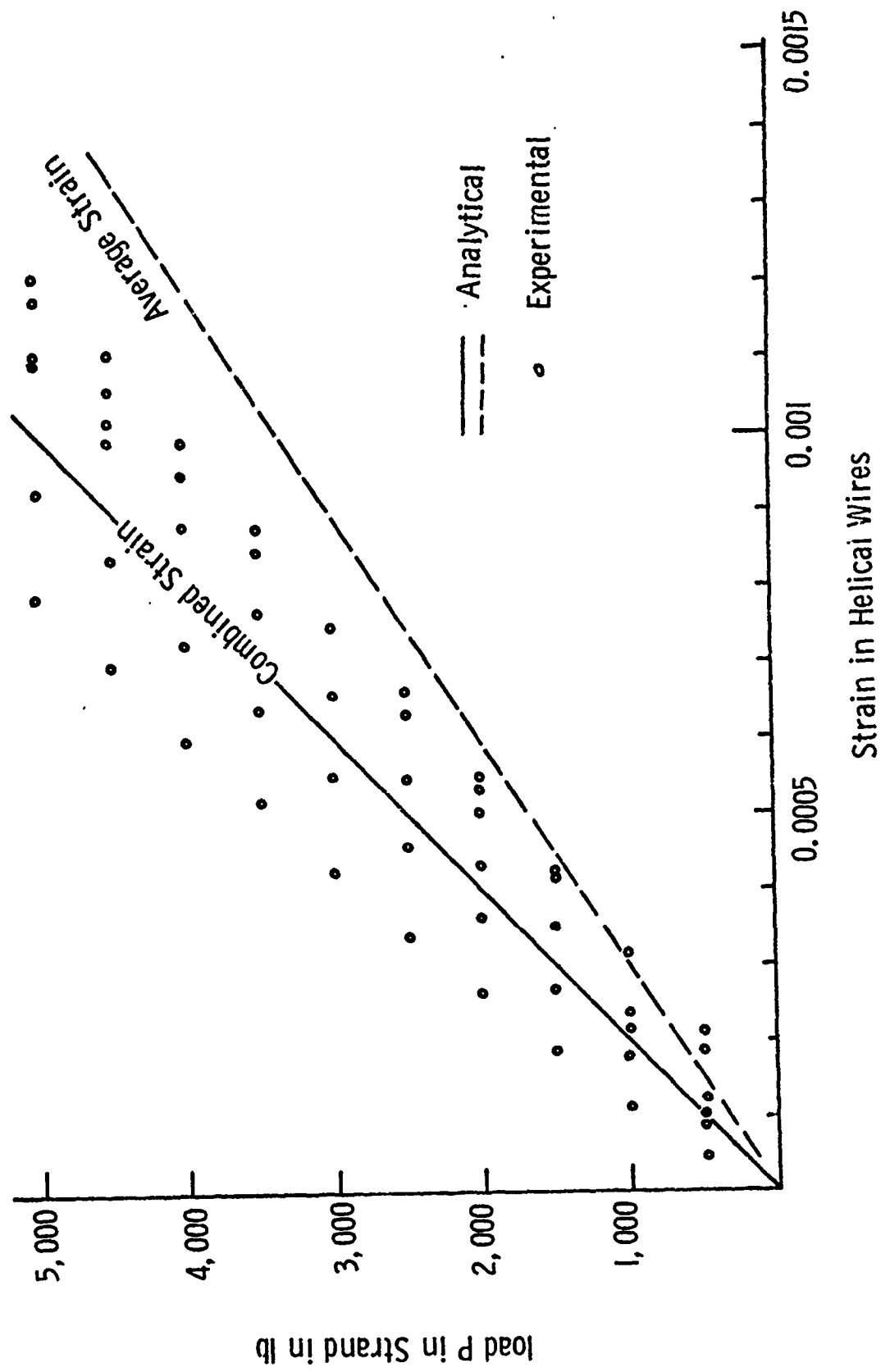


Fig. 5 Load vs. Strain in Helical Wires of a 5/16 in. Strand with Free-End



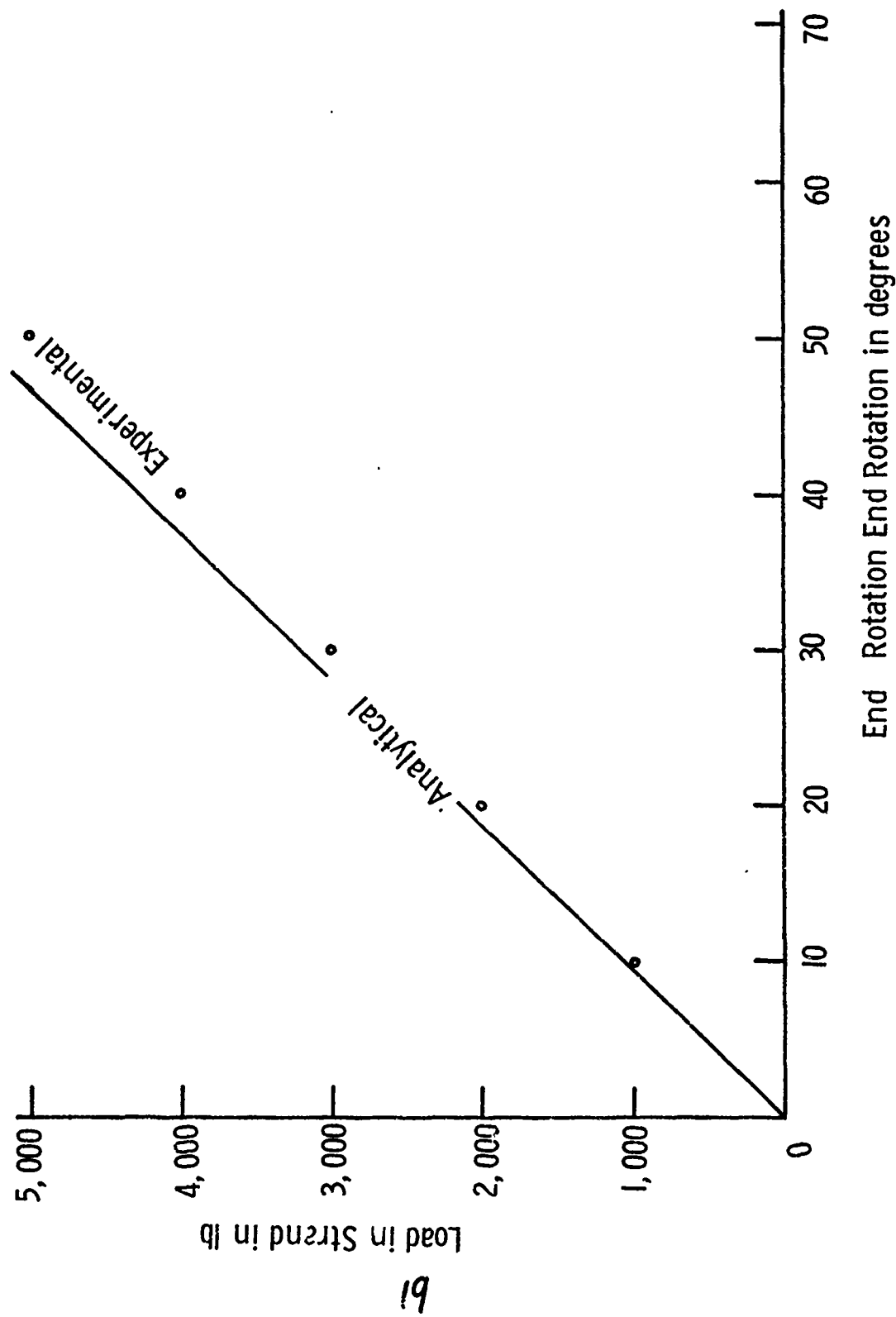
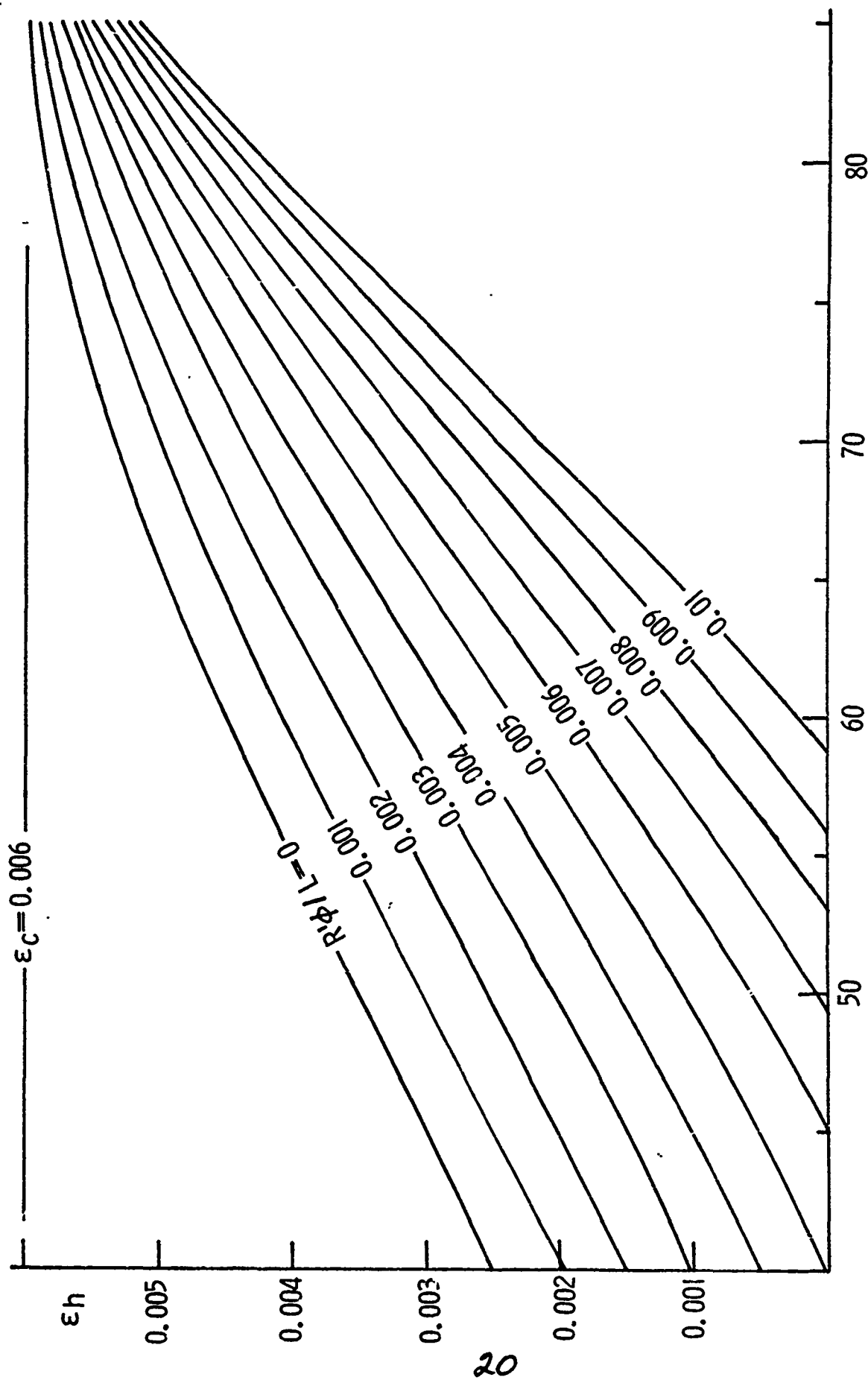


Fig. 6 Load vs. End Rotation in a 5/16-in. Strand with Free-End



Pitch Angle,  $\alpha$ , in degrees

Fig. 7 Effect of End Rotation on  $\epsilon_h$  for different Pitch Angles for  $K_I = 1$  and  $\epsilon_c = 0.006$

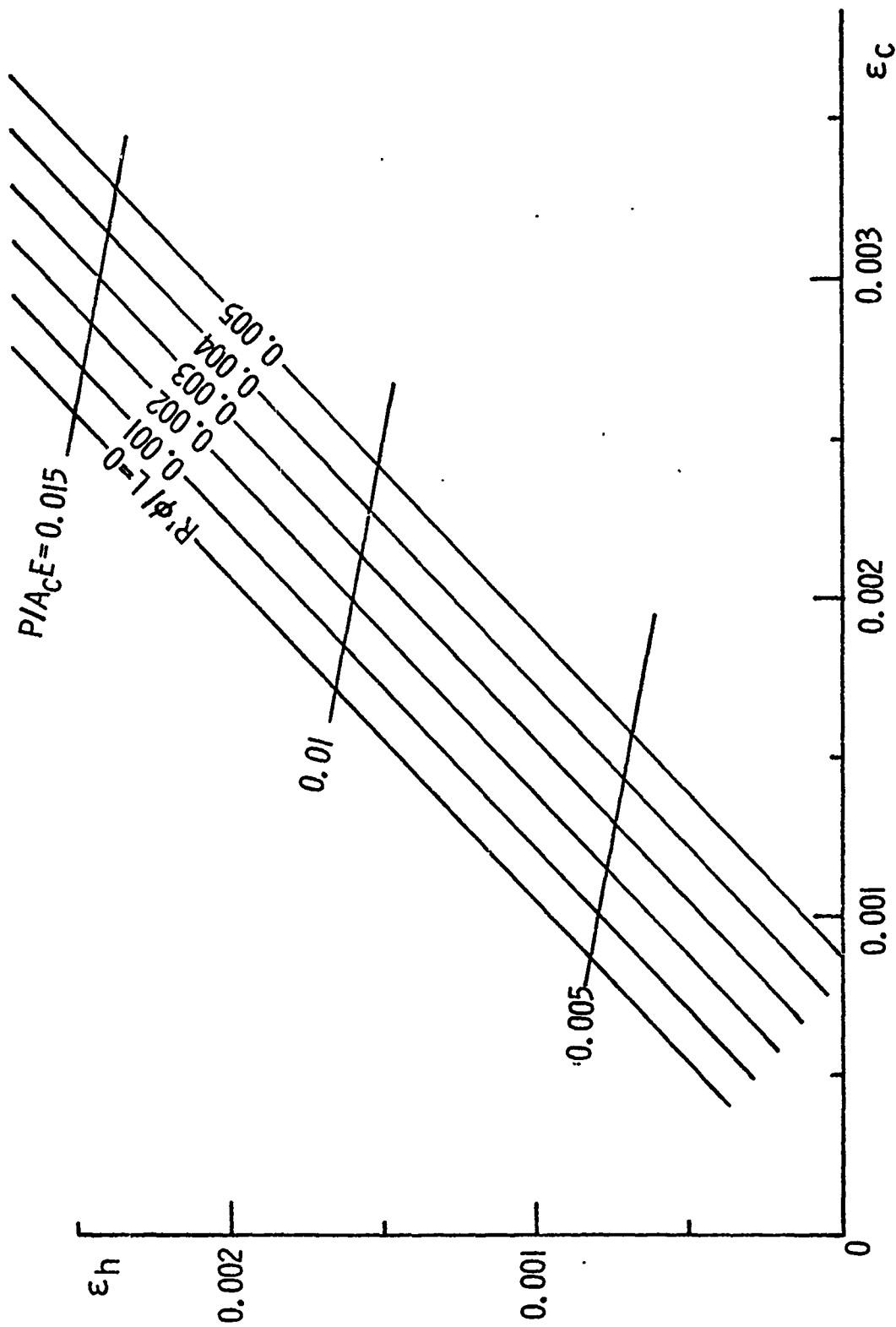


Fig. 8 Typical Variation of Strains in Wires for Different  $R'\phi/L$  and Load Levels  
for  $K_1=1$ ,  $\alpha=80^\circ$  and  $NA_h/A_c = 5$

**NATIONAL TRANSPORTATION SAFETY BOARD**  
**Washington, D. C. 20591**

SA-None File No. A-0003  
**AIRCRAFT ACCIDENT REPORT**

**ALITALIA AIRLINES**  
**MCDONNELL-DOUGLAS DC-8-62, I-DIWZ**  
**(ITALIAN REGISTRY)**  
**JOHN F. KENNEDY INTERNATIONAL AIRPORT**  
**JAMAICA, NEW YORK**  
**SEPTEMBER 15, 1970**  
**Adopted: APRIL 28, 1971**

E R R A T A

The following changes should be made to the subject report:

Page 10, column 1, lines 10 - 12 delete "at a point approximately 0.1 mile before reaching the outer marker (approximately 2.9 miles from the end of the runway)." and insert: "at a point approximately 2.8 miles from the end of the runway."

Page 11, column 2, (b) Probable Cause, Line 6 insert: "high" following "... uncorrectable".

**REPORT NUMBER: NTSB AAR-71-9**

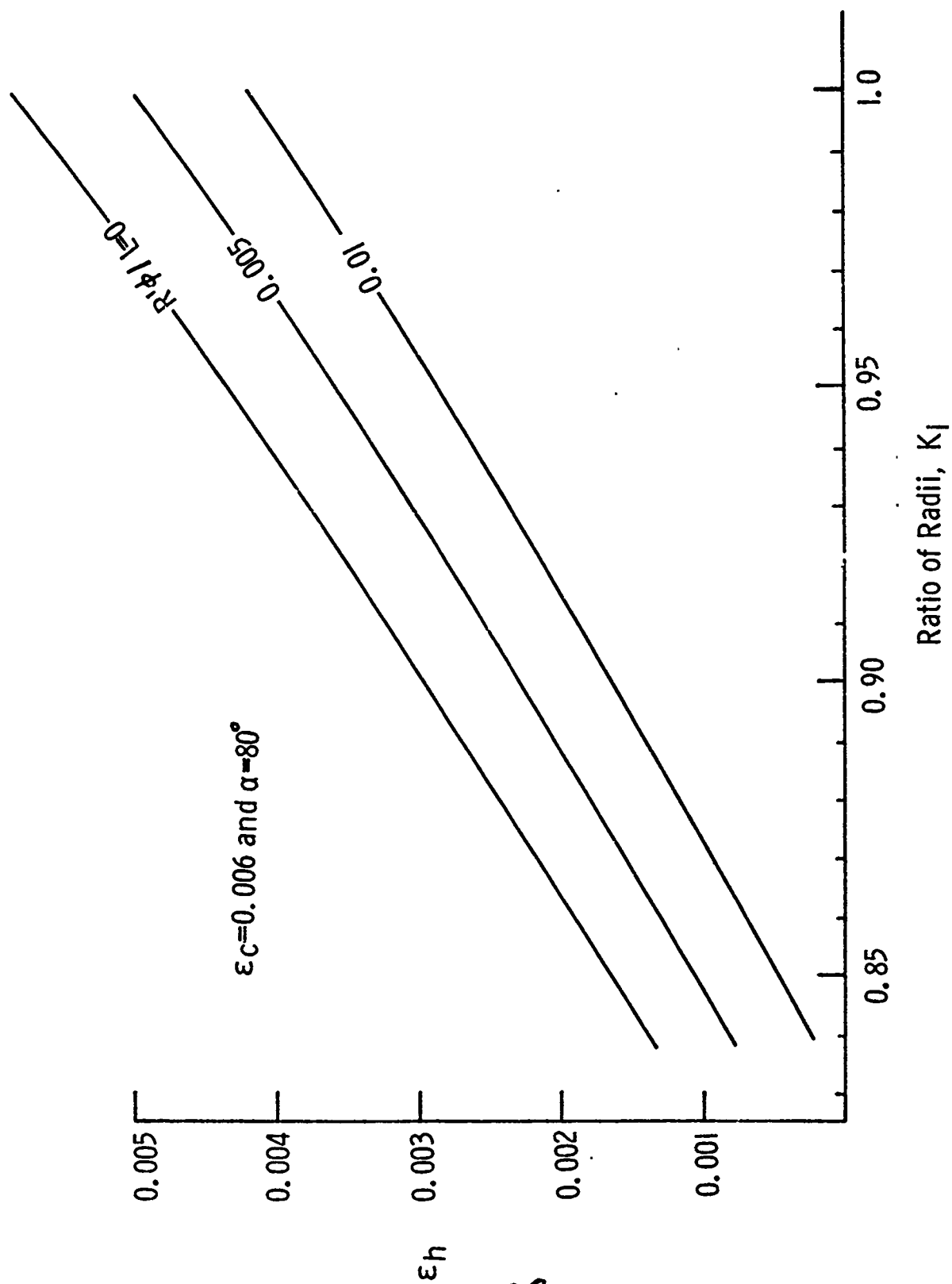


Fig. 9 Effect of Reduction of Radius on  $\epsilon_h$  For Different  $R'\phi/L$

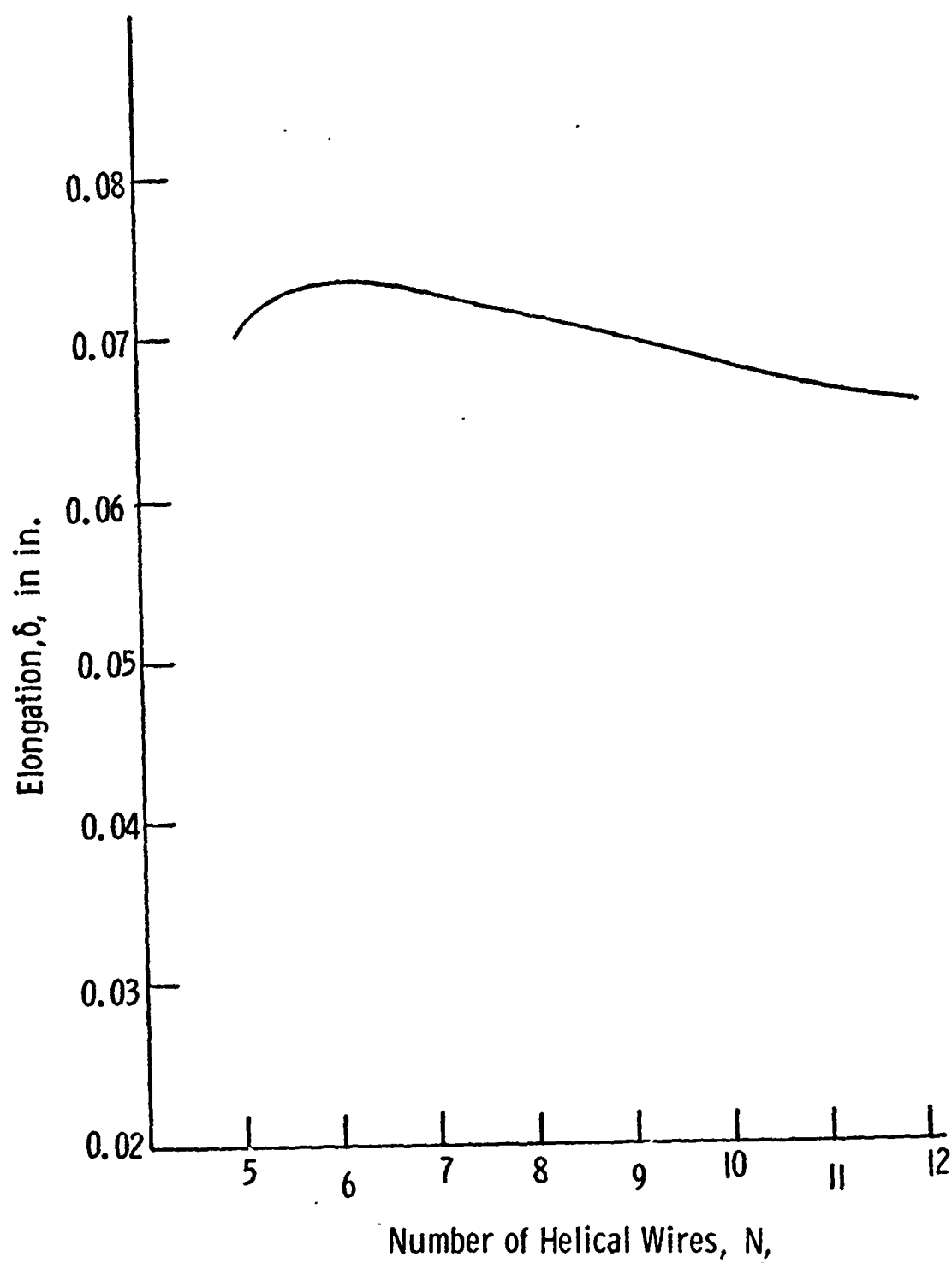


Fig. 10 Elongation of Strand for Different constructions

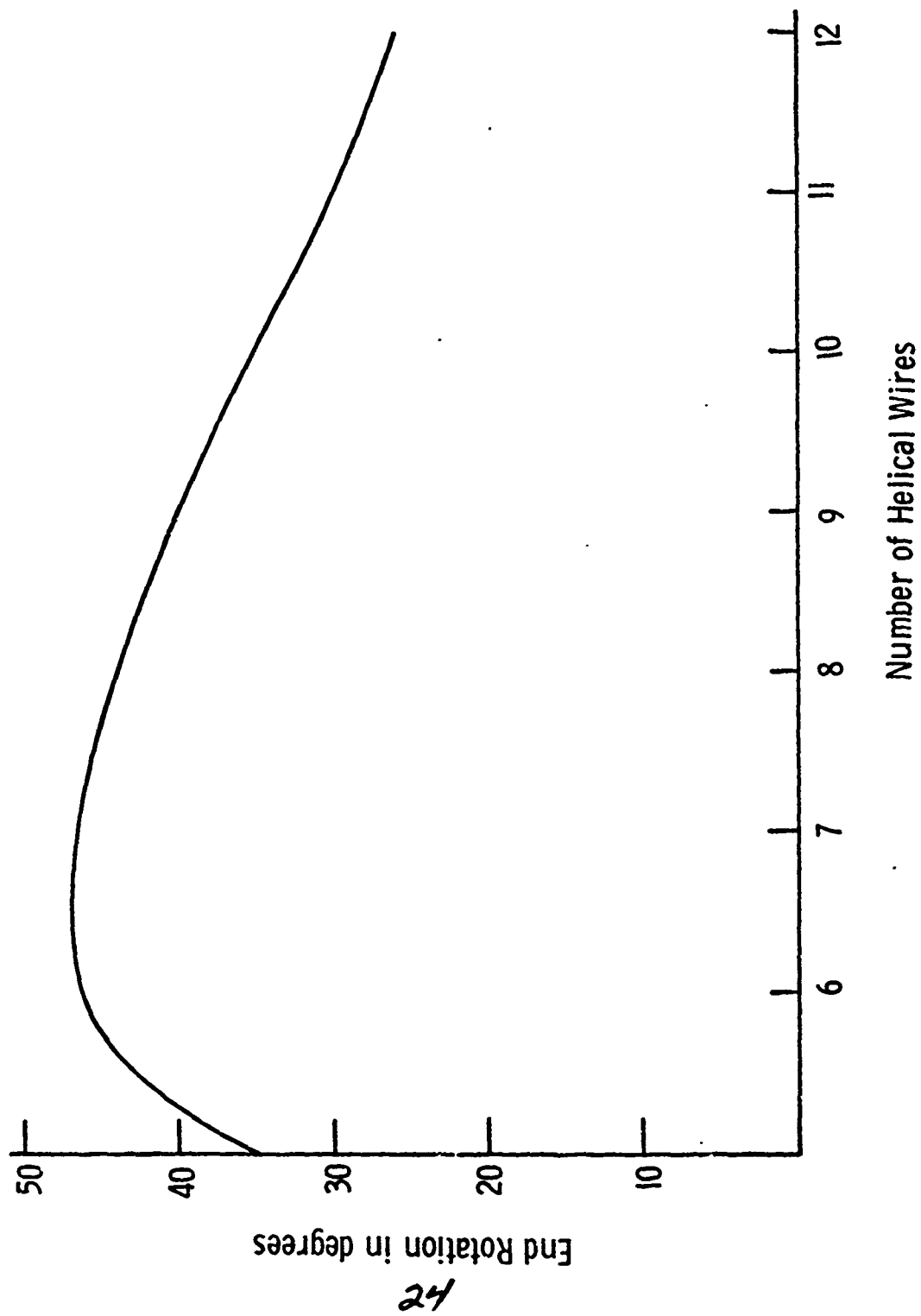


Fig. 11 End Rotation for Different Constructions